Dissection of the pH Dependence of Inhibitor Binding Energetics for an Aspartic Protease: Direct Measurement of the Protonation States of the Catalytic Aspartic Acid Residues[†,‡]

Dong Xie,* Sergei Gulnik, Laura Collins, Elena Gustchina, Leonid Suvorov, and John W. Erickson*

Structural Biochemistry Program, SAIC Frederick, National Cancer Institute−Frederick Cancer Research and Development Center, Frederick, Maryland 21702-1201

Received June 27, 1997; Revised Manuscript Received October 2, 1997[⊗]

ABSTRACT: The catalytic activity and inhibitor binding energetics of enzymes are often pH-dependent properties. Aspartic proteases comprise an important class of enzyme targets for structure-based drug design. We have performed a complete thermodynamic study of pepstatin binding to plasmepsin II, an aspartic proteinase found in *Plasmodium falciparum*, using isothermal titration calorimetry and circular dichroism. Thermodynamic parameters (ΔG, ΔH, ΔC_p, and ΔS) were measured as functions of both pH and temperature. In the pH range from 4.5 to 7.0, pepstatin binding is accompanied by proton transfer between the solvent and the complex. We used thermodynamic proton linkage theory to derive both the pH-independent binding energetics for pepstatin and the number and pK_a values of ionizable residues whose pK_a values change during ligand binding. These residues were identified as the two catalytic aspartates, with pK_as of 6.5 and 3.0, and His 164, with a pK_a of 7.5, based on the three-dimensional structure of the pepstatin−plasmepsin II complex. At pH 5.0, where the protease has optimum activity, the proton transfer process contributes almost 40% of the total binding free energy change and the total charge of the active-site aspartic acid residues is −1. These experimental results provide direct measurement for the protonation states of the catalytic aspartates in the presence of bound ligands. Comparison of the thermodynamic and structural data for pepstatin binding with human cathepsin D, a lysosomal aspartic protease that shares 35% sequence identity with plasmepsin II, suggests that the energetic differences between these two proteins are due to a higher interdomain flexibility in plasmepsin II.

The emergence of drug-resistant forms of malarial parasites demands new chemotherapeutic strategies for combating this widespread disease. Plasmepsin II from *Plasmodium falciparum*, the most virulent strain of the malarial parasite, is an aspartic protease involved in the hemoglobin degradation pathway (*1*). It thus provides a novel target for antimalarial agents. The three-dimensional structure of plasmepsin II in a complex with pepstatin A has been determined by X-ray crystallography, and on the basis of the structure a series of inhibitors have been described (*2*). The interactions between pepstatin and plasmepsin II are similar to those observed for other aspartic proteases, such as cathepsin D (*3*) and endothiapepsin (*4*). However, isothermal titration calorimetry (ITC)[1] studies indicate that pepstatin binding to these enzymes exhibits different energetic mechanisms (*5*). From the standpoint of structure-based drug design, it is important to determine contributions from all the forces involved in inhibitor binding, including the energy associated with protonation.

For aspartic proteases, it is well-established that both substrate catalysis and inhibitor binding are pH-dependent processes (*6*−*10*). Changes in the ionization state of the two catalytic aspartic acid residues have been proposed to be responsible for this pH dependency. To address these questions, we performed a detailed thermodynamic characterization of pepstatin binding to plasmepsin II over the pH range 4.5−7.0 using ITC. The pH-independent intrinsic binding energetics and the charge state of the ionizable groups involved in inhibitor binding were determined using a statistical thermodynamic approach. Comparison of the thermodynamic parameters associated with pepstatin binding for plasmepsin II with those of cathepsin D reveals differences that are predictive of structural changes induced upon inhibitor binding.

MATERIALS AND METHODS

Plasmepsin II Purification and Activation. A plasmid containing the gene encoding proplasmepsin II in a PET 22B vector (Novagen) was a kind gift of Dr. D. Goldberg (Washington University, St. Louis). Protein expression, purification, and activation were performed as described (*2*).

Isothermal Titration Calorimetry. Inhibitor binding was measured with an Omega titration microcalorimeter (Microcal, Northampton, MA) whose design and operation have been described previously (*11*). Protein solutions were

[†] This research is supported by the National Cancer Institute under Contract NO1 CO-56000.

[‡] The content of this publication does not necessarily reflect the views or policies of the Department of Health and Human Services, nor does mention of trade names, commercial products, or organization imply endorsement by the U.S. Government.

* To whom correspondence should be addressed: Structural Biochemistry Program, SAIC Frederick, National Cancer Institute−Frederick Cancer Research and Development Center, Bldg 322, Rm. 27C, Frederick, MD 21702. Tel (301) 846-1954; Fax (301) 846-6066; email xie@ncifcrf.gov.

[⊗] Abstract published in *Advance ACS Abstracts,* December 1, 1997.

[1] Abbreviations: ITC, isothermal titration calorimetry; UV, ultraviolet; CD, circular dichroism; ASA, solvent-accessible surface area; NMR, nuclear magnetic resonance.

S0006-2960(97)01550-X CCC: $14.00

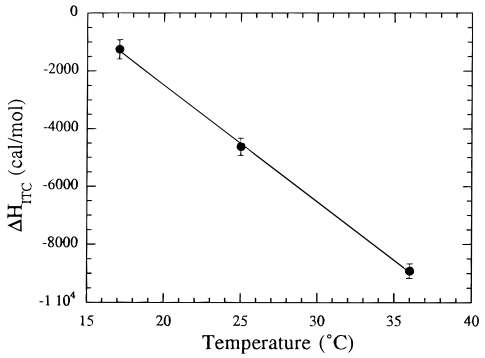

FIGURE 1: Binding enthalpy of pepstatin−plasmepsin II association as a function of temperature. The buffer was 10 mM acetate, pH 5.5. The ΔC_p value determined from the linear fitting, represented by the slope of the solid line, was −400 ± 10 cal/(mol·K).

prepared by dialysis against 10 mM desired buffer at 4 °C. Protein concentrations were determined by measuring optical absorbance at 280 nm using an extinction coefficient of 1.024 $(\text{cm·mg/mL})^{-1}$ for plasmepsin II and 1.1 $(\text{cm·mg/mL})^{-1}$ for cathepsin D. A concentrated stock solution of pepstatin A (Sigma, St. Louis, MO) was prepared in water at pH 11.5. All protein and inhibitor samples were degassed for 15 min prior to use. Reaction heats were determined after repeated injections of a fixed amount of pepstatin A into a solution of plasmepsin II. The solution was stirred at a rate of 400 rpm. The heat of dilution for pepstatin, which has been shown to be concentration-independent, was determined by taking the average of the last three injections after the protein was saturated with inhibitor.

Statistical Thermodynamic Analysis. Nonlinear least-squares analysis was performed using the program NONLIN developed by Dr. Michael Johnson at University of Virginia. This program implements a modified Gauss−Newton nonlinear least-squares algorithm for the determination of the most probable model parameters (*12*, *13*). Confidence intervals of the fitted parameters were estimated assuming a confidence level of 68.9% for the experimental data.

Circular Dichroism. CD spectra were measured with a Jasco J-720 spectropolarimeter. Each sample was scanned three times using a 0.2 mm cylindrical cell.

RESULTS

Isothermal Titration Calorimetry. In order to obtain a complete temperature profile of the thermodynamic parameters associated with pepstatin binding to plasmepsin II, we performed ITC experiments over the temperature range 17−36 °C. Figure 1 shows the binding enthalpy as a function of temperature at pH 5.5. Over a narrow temperature range, the temperature dependence of ΔH can be described by

$$\Delta H_{\text{ITC}} = \Delta H_0 + \Delta C_p(T - T_0) \qquad (1)$$

where ΔH_0 is the binding enthalpy at an arbitrary reference temperature T_0, and ΔC_p is the heat capacity change of binding. Thus the ΔC_p value determined from the slope of the linear fit in Figure 1 was −400 cal/(mol·K), which is typical for protein−peptide (*14*, *15*) and antibody−antigen interactions (*16*).

The reaction enthalpy determined from a single calorimetry experiment contains contributions from the intrinsic binding enthalpy of the reactants and also depends on the ionization enthalpy of the buffer used in the experiment (*10*, *14*). When

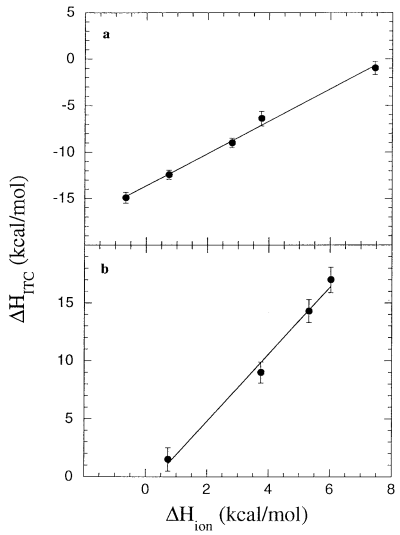

FIGURE 2: Calorimetry-measured enthalpy as a function of buffer ionization enthalpy at pH 6.5 and 36 °C. According to eq 2, Δn and $\Delta H_{\text{binding}}$ were determined to be 1.7 ± 0.1 and −13.6 ± 0.3 kcal/mol for pepstatin−plasmepsin II binding (a) and 2.9 ± 0.2 and −1.0 ± 0.8 kcal/mol for pepstatin−cathepsin D association (b). The buffers used and their ionization enthalpies are listed in the footnote of Table 1.

inhibitor binds at a constant pH, a change in the pK_a of any ionizable groups involved in inhibitor binding will result in proton transfer between the binding complex and the buffer molecules. Consequently, the calorimetrically measured enthalpy is buffer-dependent and can be represented by

$$\Delta H_{\text{ITC}} = \Delta H_{\text{binding}} + \Delta n \Delta H_{\text{ion}} \qquad (2)$$

where Δn is the number of transferred protons upon binding, ΔH_{ion} is the ionization enthalpy of buffer, and $\Delta H_{\text{binding}}$ is the buffer-independent binding enthalpy. It should be noted that Δn is positive when protons are transferred to the binding complex from the solvent, and vice versa. If there is no proton transfer, then $\Delta H_{\text{ITC}} = \Delta H_{\text{binding}}$. Figure 2 shows the calorimetric enthalpy for pepstatin A binding to plasmepsin II and cathepsin D measured in different buffers at pH 6.5 and 36 °C. For the association of pepstatin with plasmepsin II, 1.7 protons were transferred to the binding complex and $\Delta H_{\text{binding}}$ was determined to be −13.6 kcal/mol. In the case of cathepsin D, the binding of pepstatin was characterized by a Δn of 2.9 and $\Delta H_{\text{binding}}$ of −1.0 kcal/mol under the same conditions.

The major goal of this study was to characterize the pH dependence of inhibitor binding energetics for an aspartic protease. We therefore carried out ITC measurements of the binding of pepstatin A to plasmepsin II over the pH range 4.5−7.0. The pH dependence of the buffer-independent thermodynamic parameters (i.e., Δn, $\Delta H_{\text{binding}}$, and K_d), defined using eq 2, is plotted in Figure 3 and listed in Table 1.

Statistical Thermodynamic Analysis of pH Dependence of Binding Energetics. At pH 4.5, the association of pepstatin and plasmepsin II has a Δn value of −0.3. This indicates, in the simplest case, release of a proton due to decrease in the pK_a of a single ionizable group. On the other hand, Δn is 1.7 at pH 6.5, indicating the protonation of at least two ionizable groups whose pK_a values increase when pepstatin binds. Taken together, there must be at least three ionizable groups whose pK_as are altered upon pepstatin binding. The

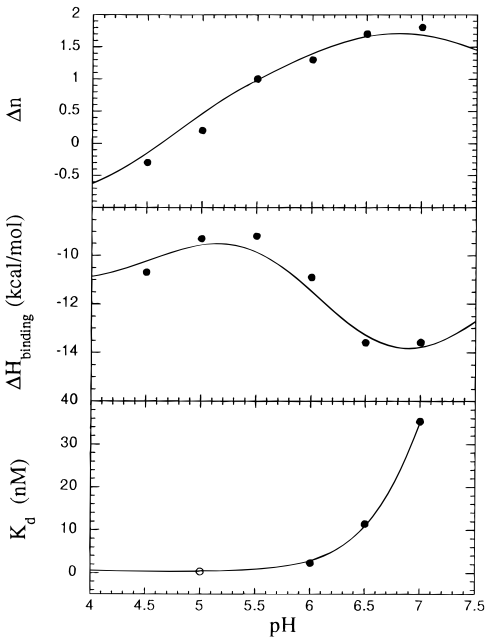

FIGURE 3: pH dependence of the buffer-independent thermodynamic parameters for pepstatin−plasmepsin II association. Δn and $\Delta H_{binding}$ are defined in eq 2. K_d represents the inhibitor dissociation constant. The K_d value at pH 5.0, represented by an open circle, was the value of K_i determined by enzymatic assay (L.S. and S.G., unpublished results). The solid lines represent fitting curves using eqs 3−5.

Table 1: Buffer-Independent Thermodynamic Parameters of Pepstatin−Plasmepsin II Binding Measured by Isothermal Titration Calorimetry at 36 °C[a]

pH	Δn	$\Delta H_{binding}$ (kcal/mol)	ΔC_p [cal/mol·K]	ΔG_b (kcal/mol)	K_d[b] (nM)
4.5	-0.3 ± 0.1	-10.7 ± 0.2	−450		nd
5.0	-0.2 ± 0.1	-9.3 ± 0.3	nd	−13.5	0.3[c]
5.5	1.0 ± 0.1	-9.2 ± 0.3	−400		nd
6.0	1.3 ± 0.2	-10.9 ± 0.5	−550	−12.2	2.3
6.5	1.7 ± 0.1	-13.6 ± 0.3	−670	−11.2	11 ± 5
7.0	1.8 ± 0.1	-13.6 ± 0.3	nd	−10.5	35.3 ± 4.2

[a] Δn and $\Delta H_{binding}$ are defined in eq 2. The errors were determined from the linear fittings as shown in Figure 2. The buffers (sodium salt) and their ionization enthalpies (in kilocalories per mole) at 36 °C are as follows: citric acid, −0.8; acetate, −0.2; MES, 3.8; maleic acid, −1.1; glycerol 2-phosphate, −0.6; ACES, 7.4; PIPES, 2.8; phosphate, 0.7; Cacodylate, −0.7; and MOPS, 5.3. nd, not determined. [b] K_d was determined by the analysis of ITC data. The value of K_d at pH 6.0 was too low to be measured accurately by calorimetry. The number in the table was obtained by a nonlinear least-squares fitting of the binding isotherm at pH 6.0. It provides a higher limit of K_d. [c] The K_d value at pH 5.0 was the value of K_i determined by using enzymatic assay (L.S. and S.G., unpublished results).

pK_a values of these ionizable groups can be determined from a global analysis of the pH dependence of the thermodynamic parameters. The pH dependence of Δn can be represented by

$$\Delta n = \sum_i \Delta n_i = \sum_i \left(\frac{10^{pK_{a,i}' - pH}}{1 + 10^{pK_{a,i}' - pH}} - \frac{10^{pK_{a,i} - pH}}{1 + 10^{pK_{a,i} - pH}} \right) \quad (3)$$

where Δn_i is the number of protons transferred to or from the ith ionizable group and is in the range of ± 1.0, and p$K_{a,i}$ and p$K_{a,i}'$ are the pK_as of the ith ionizable group before and after the association of pepstatin. The two terms in the parentheses represent the degree of protonation of the ith ionizable group before and after inhibitor binding. Figure 4 shows a simulated curve of Δn as a function of pH for the case in which proton transfer is due to the simultaneous pK_a change of two ionizable groups. At low pH, proton release indicated by the negative sign of Δn is due to a decrease of pK_a from 5 to 2 of the first ionizable group. At high pH values, this group remains ionized and does not contribute to Δn, while the pK_a increase from 6 to 9 of a second ionizable group results in a positive Δn, or proton uptake. Like Δn, the buffer-independent enthalpy of inhibitor binding can be described as

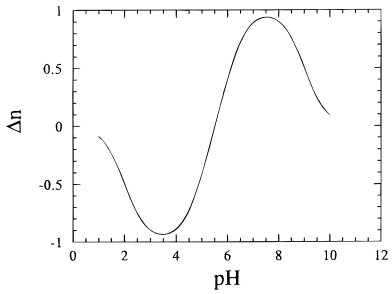

FIGURE 4: Simulated proton transfer for the binding reaction as a function of pH. The simulated proton transfer is due to pK_a change of two ionizable groups. The pK_a of the first group drops from 5 to 2, resulting in the negative Δn values at low pHs. The pK_a of the second group increases from 6 to 9, which is responsible for the proton uptake at high pHs.

$$\Delta H_{binding} = \Delta H_0 + \sum_i \Delta n_i \Delta H_i$$

$$= \Delta H_0 + \sum_i \left(\frac{10^{pK_{a,i}' - pH}}{1 + 10^{pK_{a,i}' - pH}} - \frac{10^{pK_{a,i} - pH}}{1 + 10^{pK_{a,i} - pH}} \right) \Delta H_i \quad (4)$$

where ΔH_i is the protonation enthalpy of the ith ionizable group and ΔH_0 represents the intrinsic binding enthalpy and is independent of both pH and buffer. It should be noted that if the pH is much higher than p$K_{a,i}'$ and p$K_{a,i}$, all ionizable groups will be deprotonated and ΔH_{ITC}, $\Delta H_{binding}$, and ΔH_0 will have the same value. Finally, the binding constant and ΔG are also modified by the proton transfer process as described (*17*):

$$K_b = (K_d)^{-1} = K_0 \prod_i \left(\frac{1 + 10^{pK_{a,i}' - pH}}{1 + 10^{pK_{a,i} - pH}} \right) \quad (5)$$

$$\Delta G_b = \Delta G_0 - RT \sum_i \left(\frac{1 + 10^{pK_{a,i}' - pH}}{1 + 10^{pK_{a,i} - pH}} \right) \quad (6)$$

where K_0 and ΔG_0 are the pH-independent intrinsic binding constant and free energy change, respectively, and K_d is the dissociation constant.

A nonlinear least-squares fitting program (*13*) was used to simultaneously fit Δn, $\Delta H_{binding}$, and K_d as functions of pH according to eqs 3, 4, and 5, respectively. It should be noted that at low pHs the binding constants are too high to be measured accurately by calorimetry. Although low enzyme concentration has been used to allow better measurement of the binding constant, as shown in Table 1, the error of K_d at pH 6.5 is still large. At pH 6.0, calorimetry measurement reaches its limit of sensitivity and the K_d value

Table 2: Buffer Independent Thermodynamic Parameters for Pepstatin−Plasmepsin II Association Derived from Global Analysis of the pH Dependence of Pepstatin Binding[a]

Intrinsic Binding Energetics at 36 °C			
ΔC_p	−400 ± 60 cal/(mol·K)		
ΔH_0	−9.6 ± 0.6 kcal/mol		
K_0	0.6 μM		
ΔG_0[b]	−8.8 ± 1.6 kcal/mol		
Proton Linkage Parameters			
ionizable group	1	2	3
pK_a'	6.5 ± 0.5	3.0 ± 1.5	7.5 ± 0.4
pK_a	4.7 ± 1.4	4.7 ± 1.4	6.0 ± 0.4
ΔH_i (kcal/mol)	2.1 ± 0.8	2.1 ± 0.8	−7.0 ± 0.2

[a] The errors were estimated from the confidence intervals of the fitting (Johnson & Frasier, 1985). The pK_a of groups 1 and 2 in the uninhibited enzyme were highly correlated. Hence they were fitted as one parameter as well as the protonation enthalpy. The fitted value represents only an apparent pK_a of these two groups. [b] ΔG_0 was calculated by the formula RT ln K_0, where R is the gas constant and T is the temperature.

obtained from fitting of the binding isotherm provides an upper limit of the dissociation constant. Despite the large errors of K_d at low pHs, $\Delta H_{binding}$ and Δn can be determined accurately. It was found that the results of the global analysis are essentially the same by fitting $\Delta H_{binding}$ and Δn alone and are not affected by the error of K_d. This is because a 2-fold change of K_d under these conditions reflects a ΔG_b change of only 0.3 kcal/mol. Therefore, the only parameter that is sensitive to the error of K_d is K_0, the pH-independent binding constant. The simplest model considers three ionizable groups as discussed above. In this analysis, the pK_as of two ionizable groups in the uncomplexed reactants were found to be highly correlated. Hence, their pK_a and ΔH_i values were each fit as a single parameter such that their fitted values represent their apparent properties. As shown in Figure 3, the calculated curves are in good agreement with the experimental data and were used to derive the pH-independent thermodynamic parameters listed in Table 2. In the following discussion, we will show that this model corresponds best with the structural information.

On the basis of the global analysis, the association of pepstatin and plasmepsin II is characterized by a favorable intrinsic enthalpy of −9.6 kcal/mol and a ΔG of −8.8 kcal/mol at 36 °C (Table 2). These values are pH-independent and correspond to the protein−inhibitor association when all three ionizable groups are deprotonated. At pH 5.0, the proton transfer process contributes −5.2 kcal/mol to ΔG according to eq 5. This energy accounts for almost 40% of the total free energy in this case and indicates the importance of taking this process into account when studying the binding mechanism and designing inhibitors. Two ionizable groups in the free enzyme have highly correlated pK_as and titrate with a single apparent pK_a of 4.7. We believe that these ionizable groups correspond to the carboxylate groups of the reactants. The pK_a and protonation enthalpy of the third ionizable group correspond to the properties of an imidazole group exposed to solvent (*18*).

Structural Analysis of pK_a Changes. To rule out the possibility of a pH-induced structural transition in the enzyme, we measured the CD spectra for plasmepsin II as a function of pH. The native enzyme exhibits identical far-UV CD spectra over the pH range 4.5−7.0 (Figure 5a), suggesting that the enzyme maintains its overall secondary structure over the pH range of our thermodynamic study.

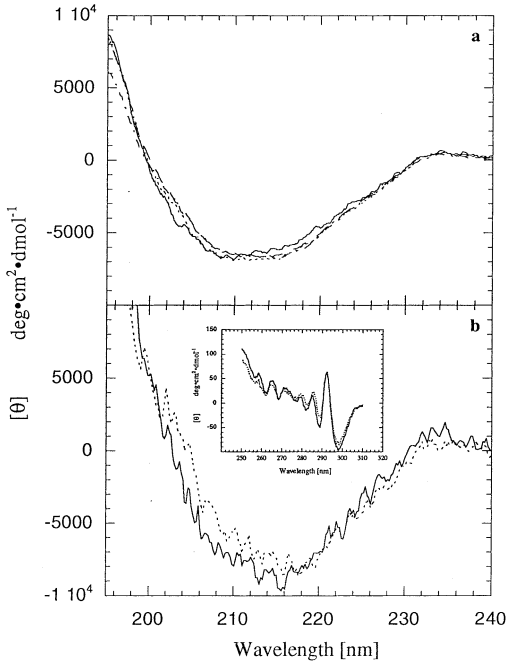

FIGURE 5: Mean residue ellipticity of plasmepsin II at 23 °C. (a) Far-UV CD spectra of uninhibited plasmepsin II at pH 4.5 (-•-), pH 6.0 (- - -), pH 6.5 (•••), and pH 7.0 (—). The protein concentrations were approximately 0.3 mg/mL. (b) Far-UV and near-UV (inset) CD spectra of uninhibited plasmepsin II (—) and plasmepsin II complexed with pepstatin (•••) at pH 6.0.

The effect of inhibitor binding was also assessed by measuring CD spectra of the plasmepsin II/pepstatin complex in both the far-UV and near-UV regions (Figure 5b). The spectra were identical to those of the uninhibited protein, indicating little change of either secondary or tertiary structure upon inhibitor binding.

According to the pK_a values in Table 2, the three ionizable groups should be exposed to solvent before binding and become buried when the binding complex is formed in order to display a pK_a shift. Since there are no major conformational changes in plasmepsin II induced by inhibitor binding as shown by the CD spectra, we hypothesized that the ionizable residues that exhibit pK_a changes are expected to be in the active-site region where they could be directly influenced by inhibitor interactions. Examination of the three-dimensional structure of the plasmepsin II−pepstatin complex (*2*) revealed only two residues, Asp34 and Asp214, that could have pK_a shifts in the pH range of our study, suggesting that the first two ionizable groups in Table 2 correspond to the catalytic carboxylate groups. The C-terminal carboxylate group of pepstatin is exposed to solvent in the complex and thus should not contribute to the observed proton transfer. It is interesting to note that the pK_as of the two aspartates change in opposite directions when pepstatin binds. Consequently, the protonation state of these two catalytic residues is −1; i.e., one is protonated and the other is ionized over the pH range studied. Similar results were obtained in a recent NMR study of the ionization states of the catalytic aspartates in a HIV-1 protease−pepstatin complex (*19*).

The third ionizable group, whose pK_a shifts from 6.0 to 7.5 upon pepstatin binding, was attributed to an imidazole group; however, there is no histidine in the active-site region. The pK_a change of this residue indicates that it should be buried and protonated in the complex. Of the seven

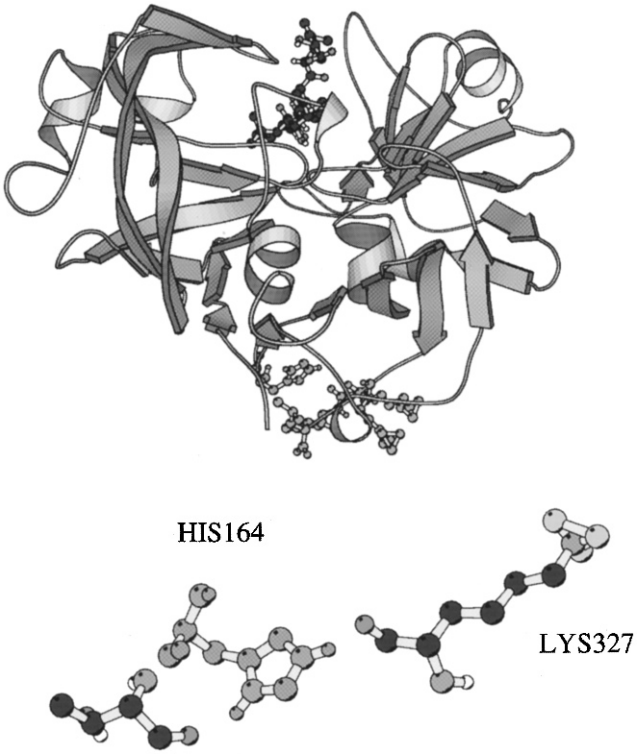

FIGURE 6: Location of His164 in plasmepsin II (upper panel). His164, in green, is located between the N-terminal and C-terminal subdomains. It is buried inside the protein by the last four residues of the C-terminus, in magenta. The Nϵ1 and Nδ2 atoms of the imidazole ring form hydrogen bonds with the carbonyl oxygens of Lys327 (2.9 Å) and Thr165 (2.8 Å), respectively (lower panel), suggesting that the imidazole group is protonated.

histidines in plasmepsin II, the only buried one is His164, which is located well outside the active site and near the end of the second strand of the six-stranded interdomain β-sheet. In the complex, the imidazole ring of His164 is covered over by the main chain of the C-terminus consisting of residues 326−329 (Figure 6). The Nϵ1 and Nδ2 atoms of the imidazole ring form hydrogen bonds with the carbonyl oxygens of Lys327 (2.9 Å) and Thr165 (2.8 Å), respectively. The aromatic ring of Tyr167 is also within 3.3 Å of Nδ2 and may form a weak hydrogen bond to this atom. These data suggest that His164 may be protonated and corresponds to the third ionizable group. According to the pK_a values determined from the ITC experiments, this residue should be more exposed to solvent in the uninhibited protein relative to the complex, where it becomes buried upon pepstatin binding and exhibits a higher pK_a. Since the CD experiments did not indicate a change in secondary or tertiary structure upon pepstatin binding, we propose that a localized conformational change affecting the environment of His164 in plasmepsin II may account for the pK_a shift of this residue.

Comparison of Inhibitor Binding to Cathepsin D and Plasmepsin II. The structures of several other aspartic proteases have been determined in complexes with pepstatin A. One of them is human cathepsin D, whose structure was recently determined (*3*, *20*). Cathepsin D exhibits 35% sequence identity to plasmepsin II. Comparison with the three-dimensional structure of plasmepsin II indicates a higher degree of homology around the active site (*2*). The observed cross-inhibition of these two enzymes by common inhibitors suggests similar inhibitor binding mechanisms (*2*). ITC was used to determine the thermodynamics of pepstatin binding to the two related enzymes (Table 3). The ΔG and ΔC_p values for pepstatin binding to the two enzymes are similar. However, the buffer-independent enthalpy, $\Delta H_{binding}$, differs by 12.6 kcal/mol for the two reactions, indicating different binding mechanisms for the two proteins. For cathepsin D, the magnitude of ΔH is small relative to that of ΔG and the binding is driven almost completely by a favorable entropy term; for plasmepsin II, on the other hand, the entropy is unfavorable and the binding is driven by a favorable enthalpy term. Furthermore, a larger value of Δn for cathepsin D indicates that there is an extra proton being transferred to the binding complex upon pepstatin binding. These results suggest that, despite the overall structural similarity of these two enzymes in the bound forms, the thermodynamic mechanism of binding differs markedly for cathepsin D and plasmepsin II.

Table 3: Structural and Thermodynamic Parameters Associated with Pepstatin Binding of Plasmepsin II and Cathepsin D

	cathepsin D	plasmepsin II
structural parameters		
buried apolar ASA[a] (Å^2)	977	934
buried polar ASA (Å^2)	386	386
configurational ΔS[b] [cal/(mol·K)]	−28.6	−27.7
thermodynamic parameters[c]		
ΔG (kcal/mol)	-10.3 ± 0.6	-11.2 ± 1.6
ΔC_p [cal/(mol·K)]	-330 ± 20	-400 ± 60
$\Delta H_{binding}$ (kcal/mol)	-1.0 ± 0.4	-13.6 ± 0.6
Δn	2.9 ± 0.1	1.7 ± 0.1

[a] ASA stands for solvent-accessible surface area. They were calculated as described (*22*) using the Lee and Richards algorithm (*39*) with a probe radius of 1.4 Å and a slice width of 0.25 Å. The calculations were performed based on the structures of cathepsin D and plasmepsin II complexed with pepstatin (*2*, 3). [b] The method of configuration entropy calculation was described in (*10*, *22*). The calculation considers entropy change due to the restriction of rotatable bonds of active site residues and pepstatin upon binding. The configurational entropy change of each residue was determined by multiplying the entropy change of freezing the side chain (*23*) by the change of degree of solvent accessibility. [c] The thermodynamic parameters were determined at pH 6.5 and 36 °C. ΔH_b and Δn are the buffer-independent binding enthalpy and the number of transferred protons defined by eq 2.

DISCUSSION

In the present study, the binding energetics of pepstatin to plasmepsin II was characterized as a function of both temperature and pH. In the pH range between 4.5 and 7.0, the binding is linked to proton transfer between the buffer and the binding complex due to pK_a shifts of three residues identified as the catalytic aspartate dyad and His164. At pH 5.0, which is the optimum pH for plasmepsin II activity, proton transfer contributes almost half of the total binding free energy. The pH-independent binding energetics is characterized by a favorable enthalpy change of 9.6 kcal/mol and a K_d of 0.6 μM.

The three-dimensional structures of cathepsin D and plasmepsin II show that the binding modes of pepstatin to these two proteins are highly similar and the binding interface of the two complexes buries almost the same amount of apolar and polar solvent-accessible surface area (ASA) at the binding interface (Table 3). It has been shown before that for protein folding or protein−peptide interactions ΔH

and ΔC_p can be accurately calculated from the change in ASA determined using three-dimensional structures (*10*, *21*, *22*); the error of the calculation was estimated to be 6% for ΔH and 9% for ΔC_p, respectively. These results suggest that the binding of pepstatin to these two proteases should exhibit similar enthalpy and heat capacity changes. We also calculated the configurational entropy change due to the restriction of rotatable bonds of the active-site residues and pepstatin upon binding (Table 3). The configurational entropy change of each residue was calculated by multiplying the entropy cost of freezing the side chain (*23*) by the change in the degree of solvent accessibility. An additional entropy term for freezing the backbone was considered for pepstatin. The calculations resulted in similar configurational entropy changes for the two binding processes. Therefore, in the absence of ligand-induced conformational changes in the enzymes, all the thermodynamic parameters (ΔH, ΔS, ΔG, and ΔC_p) associated with pepstatin binding are expected to be similar for cathepsin D and plasmepsin II. Indeed, the ΔG and ΔC_p values for pepstatin binding to the two enzymes are similar as measured at pH 6.5 and 36 °C. However, it is puzzling that the buffer-independent enthalpy, $\Delta H_{\text{binding}}$, exhibits a difference of 12.6 kcal/mol for the two reactions.

Since the inhibitor-binding interfaces for the two enzymes are very similar and calculations based on the crystal structures predict similar thermodynamic parameters for pepstatin binding, only two factors could be responsible for the enthalpy difference: a structural difference in the uninhibited forms of the two enzymes or a difference in the number of transferred protons upon pepstatin binding. According to the ITC experiments, 2.9 protons are transferred to cathepsin D compared to 1.7 for plasmepsin II. Since the crystal structures of both the pepstatin-bound and uninhibited forms of cathepsin D were essentially isomorphous (*3*), the protonated residues are expected to be at the inhibitor binding site. Inspection of the structures revealed four ionizable groups at the active site that could have a pK_a shift: the two catalytic aspartates (Asp33 and Asp231), His77, and Glu260. Since the pepstatin-binding interface of cathepsin D is similar to that of plasmepsin II, for which only one of the two catalytic aspartates becomes protonated upon pepstatin binding, we suggest that the protonated residues in cathepsin D correspond to His77, Glu260, and either Asp33 or Asp231. Since the two protonated residues in plasmepsin II are an aspartic acid and a histidine, the main difference in protonation enthalpy for the two enzyme complexes is due to a change in pK_a of Glu260 in cathepsin D. In the crystal structure of the complex, the carboxylate group of Glu260 is covered by the terminal isovaleryl side chain of pepstatin and is partially buried in the hydrophobic S4 pocket, consistent with it having an elevated pK_a relative to the free enzymes; a buried charged group here would be destabilizing to the structure (*24*). In solution the protonation enthalpy of a glutamic acid residue is −0.4 kcal/mol (*18*); the extra protonation site in cathepsin D can account for at most a small fraction of the enthalpy difference of 12.6 kcal/mol.

The above analysis indicates that the binding enthalpy difference between plasmepsin II and cathepsin D must be due mainly to a structural variation between the uninhibited enzymes. Cathepsin D has been shown to exhibit a negligible conformational change upon pepstatin binding, except for the flap movement commonly observed for aspartic proteases (*3*). Thus, we are forced to conclude that there must be a structural change between the inhibitor-bound and uninhibited forms of plasmepsin II. This conclusion agrees with the localized structural change in the enzyme that was postulated to account for the pK_a shift of His164 in plasmepsin II upon pepstatin binding. Consistent with these data, the two molecules in the asymmetric crystal unit of plasmepsin II also show a high degree of interdomain flexibility (*2*). Hence, both the thermodynamic and structural data indicate that the energetic difference between cathepsin D and plasmepsin II for pepstatin binding could be accounted for by an intersubdomain movement in plasmepsin II. Although aspartic proteases do not typically show major structural changes upon inhibitor binding, subdomain movements have been reported for endothiapepsin (*25*) and renin (*26*, *27*). According to the calorimetry data, the enthalpy change of this interdomain movement is about −12.6 kcal/mol. The favorable enthalpy must be compensated by a loss of entropy, resulting in a similar total binding free energy change as that of cathepsin D, in which only a minor interdomain movement is observed when pepstatin binds (*28*). This type of thermodynamic response is typical of the formation of polar interactions, e.g., hydrogen-bond formation in the process of protein folding or protein−peptide association (*29*−*31*). Therefore, from an energetic standpoint, the subdomain movement in plasmepsin II that accompanies pepstatin binding is characterized by the formation of new polar interactions within the protein and is presumably stabilized by the protonation of His164 and the concomitant formation of hydrogen bonds that bridge the N- and C-domains (Figure 6).

Determining the protonation state of the active-site catalytic residues is crucial for accurate calculations of inhibitor binding free energy, and ultimately for de novo inhibitor design. For the association of pepstatin with plasmepsin II, the two catalytic aspartic acid residues have different charge states in the bound complex; i.e., one is protonated and the other is ionized. For cathepsin D, 2.9 protons were transferred to the binding complex when pepstatin binds at pH 6.5. The presence of four ionizable groups, the two catalytic aspartic acid residues, His77, and Glu260, and the high degree of active-site homology with plasmepsin II suggest that the three protonated groups belong to His77, Glu260, and one of the catalytic aspartates, whose pK_a increases when inhibitor binds. The second catalytic aspartate would remain ionized at this pH. On the basis of these results, we conclude that for the cathepsin D/pepstatin complex the charge state of the two catalytic aspartates is again −1. Is this a common behavior of aspartic proteases? A microcalorimetry study of endothiapepsin showed that 1.1 protons were transferred to the complex upon the association of pepstatin at pH 7.0 (*10*). Although four aspartates of endothiapepsin are involved in the binding (*4*), only the two catalytic aspartates, Asp32 and Asp215, make polar contacts with the inhibitor and therefore could have pK_a changes and accept the transferred protons. Since 1.1 protons were transferred to the binding complex at pH 7.0, one of the catalytic aspartates must become protonated upon inhibitor binding, consistent with a −1 charge state of the active site. Recently, NMR methods were used to determine the ionization states of the catalytic aspartates in HIV-1 protease (*19*). These two residues were found to have pK_as above 6.5 for Asp25 and below 2.5 for Asp125 when pepstatin is bound.

In the uninhibited enzyme, both carboxylates are ionized at pH 6 and titrate as a single group. These properties are remarkably similar to those of the active-site carboxylates of plasmepsin II, and indicate that the ionization state of the active site dyad is also −1. These studies suggest a common thermodynamic behavior for the catalytic carboxylates of aspartic proteases. Taken together, the thermodynamic and structural data suggest that the two catalytic aspartates of aspartic proteases have different ionization states in complex with pepstatin-like inhibitors, consistent with the proposed catalytic mechanism of aspartic proteases (*32*).

Is this behavior of aspartic proteases dependent on the nature of bound inhibitor? NMR studies suggested that the ionization state of HIV PR is −1 in a complex with KNI-272, which contains a norstatine moiety as the transition-state isostere (*33*). However, care should be taken in extending these studies to other inhibitors. For instance, NMR studies of the cyclic urea, DMP-323, complexed with HIV PR suggest that both Asp25 and Asp125 are protonated in the complex leading to a neutral active site (*34*). Molecular dynamics studies suggest that the charge state of the active site of HIV PR depends on the nature of the active-site transition-state isostere (*35*).

Recently, ITC has been extensively used to study molecular interactions [see reviews (*36*, *37*)]. Using this technique, the pK_a of an active-site histidine as well as the pH-independent binding energetics have been determined for the association of elastase with ovomucoid third domain (*21*) using a proton-linkage algorithm similar to the one described here (*38*). Our study indicates that ITC combined with three-dimensional structure analysis is a powerful method for obtaining information on the ionization states for protein−inhibitor complexes, for determining pK_a changes on ligand binding, and for characterizing the complete thermodynamic profile of ligand binding reactions.

ACKNOWLEDGMENT

We thank Dr. Ernesto Freire and Dr. Javier Gomez of the Biocalorimetry Center of The Johns Hopkins University for the initiation of the cathepsin D ITC experiments, Dr. Raymond Sowder for doing the amino acid analysis of pepstatin, Dr. Martin Straume for discussions on the statistical analysis, and Karen P. Lewis for proofreading the manuscript.

REFERENCES

1. Goldberg, D. E., Slater, A. F. G., Cerami, A., & Henderson, G. B. (1990) *Proc. Natl. Acad. Sci. U.S.A. 87*, 2931−2935.
2. Silva, A., Lee, A., Gulnik, S., Majer, P., Collins, J., Bhat, T., Collins, P., Cachau, R., Luker, K., Gluzman, I., Francis, S., Oksman, A., Goldberg, D., & Erickson, J. (1996) *Proc. Natl. Acad. Sci. U.S.A. 93*, 10034−10039.
3. Baldwin, E. T., Bhat, T. N., Gulnik, S., Hosur, M. V., Sowder, R. C., II, Cachau, R. E., Collins, J., Silva, A. M., & Erickson, J. (1993) *Proc. Natl. Acad. Sci. U.S.A. 90*, 6796−6800.
4. Bailey, D., Cooper, J., Tickle, I., Veepandian, B., Blundell, T., Atrash, B., Jones, D., & Szelke, M. (1993) *Biochem. J. 289*, 363−371.
5. Xie, D., Gulnik, S., Collins, L., Gustchina, E., Bhat, T. N., & Erickson, J. W. (1997) in *Structure and Function of Aspartic Proteinases: Retroviral and Cellular Enzymes* (James, M., Ed.) Plenum, New York (in press).
6. Fruton, J. S. (1976) *Adv. Enzymol. Relat. Areas Mol. Biol. 44*, 1−36.
7. Hofmann, T., Hodges, R., & James, M. (1984) *Biochemistry 23*, 635−643.
8. Hyland, L., Tomaszek, T., & Meek, T. (1991) *Biochemistry 30*, 8454−8463.
9. Lin, Y., Fusek, M., Lin, X., Hartsuck, J., Kezdy, F., & Tang, J. (1992) *J. Biol. Chem. 267*, 18413−18418.
10. Gomez, J., & Freire, E. (1995) *J. Mol. Biol. 252*, 337−350.
11. Wiseman, T., Williston, S., Brandt, J., & Lin, L. (1989) *Anal. Biochem. 179*, 131−135.
12. Johnson, M. L. (1983) *Biophys. J. 44*, 101−106.
13. Johnson, M. L., & Frasier, S. G. (1985) *Methods Enzymol. 117*, 301−342.
14. Murphy, K. P., Xie, D., Garcia, K. C., Amzel, L. M., & Freire, E. (1993) *Proteins: Strutct., Funct., Genet. 15*, 113−120.
15. Mandiyan, V., O'Brien, R., Zhou, M., Margolis, B., Lemmon, M., Sturtevant, J., & Schlessinger, J. (1996) *J. Biol. Chem. 271*, 4770−4775.
16. Schwarz, F., Tello, D., Goldbaum, F., Mariuzza, R., & Poljak, R. (1995) *Eur. J. Biochem. 228*, 388−394.
17. Tanford, C. (1970) *Adv. Protein. Chem. 24*, 1−95.
18. Christensen, J. J., Hansen, L. D., & Izatt, R. M. (1976) *Handbook of Proton Ionization Heats and Related Thermodynamic Quantities*, John Wiley and Sons, New York.
19. Smith, R., Brereton, I., Chai, R., & Kent, S. (1996) *Nat. Struct. Biol. 3*, 946−950.
20. Metcalf, P., & Fusek, M. (1993) *EMBO J. 12*, 1293−1302.
21. Baker, B., & Murphy, K. (1996) *J. Mol. Biol. 268*, 557−569.
22. Xie, D., & Freire, E. (1994) *J. Mol. Biol. 242*, 62−80.
23. Lee, K. H., Xie, D., Freire, E., & Amzel, L. M. (1994) *Proteins: Struct., Funct., Genet. 20*, 68−84.
24. Langsetmo, K., Fuchs, J., Woodward, C., & Sharp, K. (1991) *Biochemistry 30*, 7609−7614.
25. Sali, A., Veerapandian, B., Cooper, J., Moss, D., Hofmann, T., & Blundell, T. (1992) *Proteins: Struct., Funct., Genet. 12*, 158−170.
26. Rahuel, J., Priestle, J., & Grutter, M. (1991) *J. Struct. Biol. 107*, 227−236.
27. Tong, L., Pav, S., Lamarre, D., Pilote, L., LaPlante, S., Anderson, P., & Jung, G. (1995) *J. Mol. Biol. 250*, 211−222.
28. Erickson, J. W., Baldwin, E. T., Bhat, T. N., & Gulnik, S. (1995) in *Aspartic Proteinases: Structure, Function, Biology, and Biomedical Implications* (Takahashi, K., Ed.), Plenum, New York.
29. Murphy, K. P., & Freire, E. (1992) *Adv. Protein Chem. 43*, 313−361.
30. Habermann, S., & Murphy, K. (1996) *Protein Sci. 5*, 1229−1239.
31. Kato, Y., Conn, M., & Rebek, J. J. (1995) *Proc. Natl. Acad. Sci. U.S.A. 92*, 1208−1212.
32. Suguna, K., Padlan, E., Smith, C., Carlson, W., & Davies, D. (1987) *Proc. Natl. Acad. Sci. U.S.A. 84*, 7009−7013.
33. Wang, Y., Freedberg, D., Yamazaki, T., Wingfield, P., Stahl, S., Kaufman, J., Kiso, Y., & Torchia, D. (1996) *Biochemistry 35*, 9945−9950.
34. Yamazaki, T., Nicholson, L., Torchia, D., Wingfield, P., Stahl, S., Kaufman, J., Eyermann, C., Hodge, N., Lam, P., Ru, Y., Jadhav, P., Chang, C.-H., & Weber, P. (1994) *J. Am. Chem. Soc. 116*, 10791−10792.
35. Harte, W. E., & Beveridge, D. L. (1993) *J. Am. Chem. Soc. 115*, 3883−3886.
36. Freire, E., Mayorga, O. L., & Straume, M. (1990) *Anal. Chem. 62*, 950A−959A.
37. Ladbury, J., & Chowdhry, B. (1996) *Chem. Biol. 3*, 791−801.
38. Baker, B., & Murphy, K. (1996) *Biophys. J. 71*, 2049−2055.
39. Lee, B., & Richards, F. (1971) *J. Mol. Biol. 55*, 379−400.

BI971550L